Earthq Eng & Eng Vib (2015) 14: 189-201 **DOI**:10.1007/s11803-015-0016-3

An analytical solution to the scattering of cylindrical SH waves by a partially filled semi-circular alluvial valley: near-source site effects

Zhang Ning[1, 2†], Gao Yufeng[1, 2‡], Yang Jie[3§] and Xu Changjie[4‡]

1. *Geotechnical Research Institute, Hohai University, Nanjing 210098, China*
2. *Key Laboratory of Ministry of Education for Geomechanics and Embankment Engineering, Hohai University, Nanjing 210098, China*
3. *Nanjing Hydraulic Research Institute, Nanjing 210024, China*
4. *Research Center of Coastal and Urban Geotechnical Engineering, Zhejiang University, Hangzhou 310058, China*

Abstract: The earth's surface irregularities can substantially affect seismic waves and induce amplifications of ground motions. This study investigates whether and how the source characteristics affect the site amplification effects. An analytical model of a line source of cylindrical waves impinging on an alluvial valley is proposed to link the source and site. The analytical solution to this problem proves one aspect of the strong effect of source on site amplification, i.e., the wave curvature effect. It is found that the site amplification depends on the source location, especially under conditions of a small source-to-site distance. Whether the displacement is amplified or reduced and the size of the amplification or reduction may be determined by the location of the source. It is suggested that traditional studies of site responses, which usually ignore the source effect, should be further improved by combining the source with site effects.

Keywords: site effects; source effects; wave function expansion method; cylindrical SH waves; wave scattering and diffraction

1 Introduction

It is well known that ground shaking can be significantly modified due to local site effects during an earthquake (Olsen *et al.*, 1995; Hough *et al*., 2010; Wang *et al*., 2013). Site amplification and spatial variation of ground motions are of particular importance for earthquake disaster mitigation and seismic design of critical structures. The physical process regarding site response predictions is traditionally divided into source-path-site. However, simultaneous considerations of source, path, and site effects have been pointed out (e.g., Sanchez-Sesma, 1987; Campillo *et al*, 1989; Boore, 2004). Recently, there has been debate on whether site effects are affected by source characteristics. Olsen (2000), Triantafyllidis *et al*. (2002), and Parvez *et al.* (2006) concluded that site effects depend not only on local soil characteristics but also on source characteristics based on finite difference methods or hybrid methods combining modal summation and finite difference, while Lozano *et al.* (2009) found that the dependence of site effects on the source characteristics is negligible by using spectral ratio techniques. Therefore, the conclusions regarding the role of the source in site responses drawn from numerical and empirical methods are totally opposite. An analytical study is needed to reveal the physical mechanism for the effects of sources on the site amplification.

The plane-wave assumption is frequently used in theoretical studies on site and topographic effects (e.g., Liu and Han 1991; Yuan and Liao 1995; Liang *et al*., 2004, 2006; Gao *et al*., 2012; Zhang *et al*., 2012a, 2012b; Yang *et al*., 2014). It is an acceptable approximation for studying waves at a significant distance from the source. If there is a nearby source, however, the assumption of plane waves is no longer appropriate. To study the influence of sources on site effects, non-plane wave fronts or the curvature of waves should be taken into account. The incidence of a line source of cylindrical

Correspondence to: Xu Changjie, Research Center of Coastal and Urban Geotechnical Engineering, Zhejiang University, Hangzhou 310058, China
Tel: +86 571 86050581; Fax: 86 571 86050581
E-mail: xucj@zju.edu.cn
†Lecturer; ‡Professor; §Engineer

Supported by: National Natural Science Foundation of China under Grant Nos. 51479050 and 51338009, National Key Basic Research Program of China under Grant No. 2015CB057901, the Public Service Sector R&D Project of Ministry of Water Resource of China under Grant No.201501035-03, the Fundamental Research Funds for the Central Universities under Grant Nos. 2013B05814, 2014B06814 and 2015B01214 and the 111 Project under Grant No. B13024
Received December 8, 2013; **Accepted** October 29, 2014

wave instead of a plane wave is an appropriate way to investigate the problems of near-source scattering (e.g., Groby and Wirgin, 2005; Smerzini *et al*., 2009; Iturraran-Viveros *et al*., 2010).

Site amplification due to irregular geological structures consists of contributions by the geometries (i.e., topographic amplification effects) and the materials (i.e., mechanical amplification effects of soils). Recently, we have proposed a V-shaped canyon model to study the effect of source on topographic amplification (Gao and Zhang, 2013), concluding that the topographic effect can be strongly affected by source locations. As an extension, this study aims to reveal whether the source locations can affect the mechanical amplification effects of irregular sites as well. Although numerical methods are more flexible in simulating earthquake wave propagation (Sanchez-Sesma, 1987; Sanchez-Sesma *et al*., 2002), they still cannot be employed in a blind way. Chaljub *et al*. (2010) has stated that "the numerical prediction of ground motion in general certainly cannot be considered a mature, push-button approach." The analytical solution based on the wave function expansion method not only can shed light on the nature of the problem but also verify numerical methods.

There are several analytical solutions to the scattering of plane SH wave scattering by simple irregular sites in the literature. The exact analytical solution to the scattering of plane SH waves by a semi-circular alluvial valley has been derived by Trifunac (1971). Later, Wong and Trifunac (1974) extended the study to a semi-elliptical alluvial valley. Todorovska and Lee (1991) obtained a solution for the scattering problem of plane SH waves induced by a shallow cylindrical alluvial valley by using a large circle assumption. Then Yuan and Liao (1995) removed the large circle approximation and derived an improved wave series solution for the same problem. Recently, Tsaur and Chang (2008) proposed a wave function series solution for the scattering problem of plane SH waves induced by a partially filled semi-circular alluvial valley. The incident wave sources, however, are not taken into account in these studies with the plane-wave assumption. As for the cylindrical SH wave cases, Luo (2008) obtained a solution to the scattering problem of a semi-circular alluvial valley. However, he did not focus on the wave curvature effects. Later, Luo and Lee (2014) studied the effect of a near-field SH line source on the soil-structure interaction problem. Here we propose an analytical solution to a simple scattering problem: that of a line source of cylindrical SH waves impinging on a soft partially filled semi-circular alluvial valley. This work aims to reveal whether, how and to what extent the source influence the site effects.

2 Model and theoretical formulations

The two dimensional (2D) model herein is shown in Figure 1, which represents a partially filled semi-circular alluvial valley with a radius of a in the half-space (identical to Tsaur and Chang (2008) except for the source of excitation). The feature sizes of the valley are its half-width b, the distance d from its surface to the ground level, its thickness h, and its central angle 2β. The entire domain is divided into two sub-regions (bedrock and alluvial valley) labeled by 1 and 2, respectively. The medium of every sub-region is assumed to be elastic, homogeneous, and isotropic. The material properties are given by shear modulus μ_j and shear wave speed c_j (the Subscript j = 1, 2 represents the Sub-regions 1 and 2, respectively). Two global systems of rectangular and polar coordinates, i.e., (x_1, y_1) and (r_1, θ_1), are first built with origins at the circle center of the boundary of the alluvial valley. The angle θ_1 is measured from the vertical y_1-axis counterclockwise towards the x_1-axis with a positive direction to the right. In Sub-region 2, the definitions of a local rectangular coordinate system (x_2, y_2) and a local polar coordinate system (r_2, θ_2) are adopted. The origins of the local coordinates are placed at the middle point of the top surface of the alluvial valley. The angle θ_2 is measured from the y_2-axis counterclockwise to the x_2-axis.

The alluvial valley is excited by a line source of harmonic SH cylindrical waves with angular frequency ω. The anti-plane motion of the medium is in the z_1-direction. The source location is represented by (r_0, θ_0) in the coordinate system (r_1, θ_1), and the dimensionless coordinate of the source is $(x_0/a, y_0/a)$ in the coordinate system (x_1, y_1). For convenience, the method of images is applied. Two local systems of polar coordinates (r_f, θ_f) and (r'_f, θ'_f) for the source and its image, respectively, are adopted. The angles θ_f and θ'_f are defined as shown in Fig. 1.

In the absence of the body force, the equation of motion (i.e., Helmholtz equation) and boundary conditions for the problem herein is the same as Tsaur and Chang (2008) (see their Eqs. (1)-(7)).

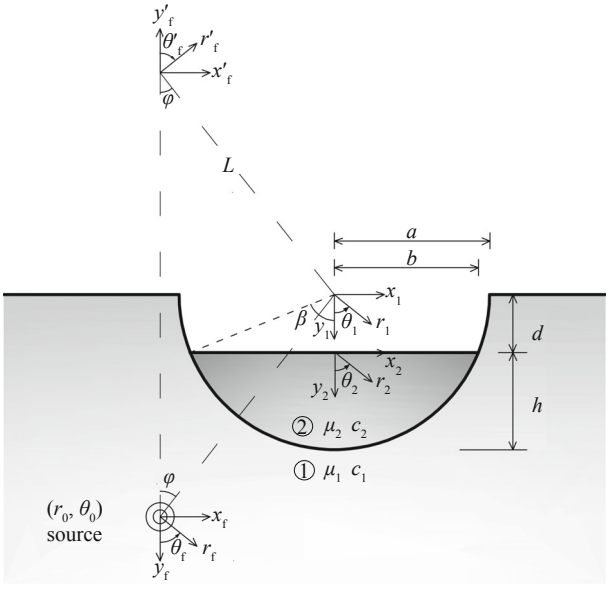

Fig.1 2D model

In Sub-region 1, the wave field can be divided into two parts. The first part is the free wave field generated by the line source in the half-space.

From the viewpoint of wave function expansion, the harmonic cylindrical wave in a full space generated by a line source can be specified by (Mow and Pao, 1971)

$$u^{\text{inc}}(r_f) = u_0 \mathrm{H}_0^{(2)}(k_1 r_{\text{f}}) \mathrm{e}^{\mathrm{i}\omega t} \tag{1}$$

where u_0 is the displacement amplitude, $k_1 = \omega / c_1$ is the wave-number, $i = \sqrt{-1}$, and $\mathrm{H}_0^{(2)}(\cdot)$ represents the second type of Hankel function of 0 order. $u^{\text{inc}}(r_{\text{f}})$ can be viewed as the incident wave for the half space. To construct the free field in the half space, the image of the line source with respect to the horizontal ground surface is employed to represent the reflection wave, i.e.,

$$u^{\text{ref}}(r_{\text{f}}') = u_0 \mathrm{H}_0^{(2)}(k_1 r_{\text{f}}') \mathrm{e}^{\mathrm{i}\omega t} \tag{2}$$

A normalization method similar to Smerzini *et al*. (2009), Iturraran-Viveros *et al*. (2010) and Gao and Zhang (2013) is used here. Normalizing the sum of Eqs. (1) and (2) to $u^{\text{inc}}(r_0)$ results in the free wave field as follows

$$u^{\text{f}} = \frac{\mathrm{H}_0^{(2)}(k_1 r_{\text{f}}) + \mathrm{H}_0^{(2)}(k_1 r_{\text{f}}')}{\mathrm{H}_0^{(2)}(k_1 r_0)} \tag{3}$$

Note that $u^{\text{inc}}(r_0)$ represents the incident-field displacement at the origin of the global coordinate system (r_1, θ_1). This normalization strategy is used so that the free-field displacement amplitude at the origin of (r_1, θ_1) due to the cylindrical-wave is identical to that associated with the unit-amplitude plane-wave (i.e., both are 2).

Suitable forms of the Graf's addition theorem (Abramowitz and Stegun, 1972; Yuan, 2014) for the problem herein have been shown as follows to achieve the transformations of coordinates from (r_{f}, θ_{f}) and (r'_{f}, θ'_{f}) to (r_1, θ_1).

$$\mathrm{H}_0^{(2)}(k_1 r_{\text{f}}) = \sum_{n=0}^{\infty} \varepsilon_n \mathrm{H}_n^{(2)}(k_1 L) \mathrm{J}_n(k_1 r_1) \cos[n(\theta_1 + \varphi)] \tag{4}$$

$$\mathrm{H}_0^{(2)}(k_1 r_{\text{f}}') = \sum_{n=0}^{\infty} \varepsilon_n \mathrm{H}_n^{(2)}(k_1 L) \mathrm{J}_n(k_1 r) \cos[n(\theta_1 - \varphi - \pi)] \tag{5}$$

where ε_n is the Neumann factor, $\mathrm{H}_n^{(2)}(\cdot)$ is the second kind Hankel function of n order, $\mathrm{J}_n(\cdot)$ is the first kind Bessel function of n order, $L = r_0$ is the distance between the origins of (r_1, θ_1) and (r_{f}, θ_{f}). The distance L and corresponding incident angle φ are depicted in Fig. 1.

Afterwards, the free wave field in (r_1, θ_1) can be obtained by putting Eqs. (4) and (5) into Eq. (3), i.e.,

$$\begin{aligned} u^{\text{f}}(r_1, \theta_1) = &\sum_{n=0}^{\infty} P_n \mathrm{J}_{2n}(k_1 r_1) \cos 2n\theta_1 + \\ &\sum_{n=0}^{\infty} Q_n \mathrm{J}_{2n+1}(k_1 r_1) \sin(2n+1)\theta_1 \end{aligned} \tag{6}$$

where the expressions of P_n and Q_n are:

$$P_n = 2\varepsilon_n \mathrm{H}_{2n}^{(2)}(k_1 L) \cos(2n\varphi) / \mathrm{H}_0^{(2)}(k_1 L) \tag{7}$$

$$Q_n = -4\mathrm{H}_{2n+1}^{(2)}(k_1 L) \sin[(2n+1)\varphi] / \mathrm{H}_0^{(2)}(k_1 L) \tag{8}$$

Similar to Smerzini *et al*. (2009), the normalization method proposed herein also allows one to establish an asymptotic equality between the plane-wave free-field and the cylindrical-wave free-field. Here is the proof.

If $L = r_0$ approaches infinity, the cylindrical wave incident angle φ herein is identical to the plane-wave incident angle α in Tsaur and Chang (2008). Then by using the following asymptotic relation for Hankel function (Abramowitz and Stegun, 1972),

$$\mathrm{H}_{\nu}^{(2)}(k_1 L) = \sqrt{2 / (\pi k_1 L)} \mathrm{e}^{-\mathrm{i}(k_1 L - \nu\pi/2 - \pi/4)}, \quad L \to \infty \tag{9}$$

we have,

$$P_n = 2\varepsilon_n (-1)^n \cos(2n\alpha), \quad L \to \infty \tag{10}$$

$$Q_n = -4\mathrm{i}(-1)^n \sin[(2n+1)\alpha], \quad L \to \infty \tag{11}$$

Thus, the cylindrical-wave free-field in this study (Eq. (6)) becomes the plane-wave free-field denoted by eq. (11) in Tsaur and Chang (2008). Equations (6)–(11) reveal theoretically the connection between the far-field plane wave and the near-source cylindrical wave used in this study. To understand the asymptotic relation numerically, one can find the effects of source distance on the cylindrical-wave free-field displacement amplitudes in Fig. 2. Figure 2(a) shows that the horizontal (φ = 90°), oblique (φ = 45°) and vertical (φ = 0°) sources are considered and the corresponding results at three different positions are given in Figs. 2(b), (c) and (d) by solid, dashed and dotted lines, respectively. To avoid potential singularities of the motions at the three positions, the range of the wave source distance is set to be from L/a = 1.1 to L/a = 100. As expected, in Figs 2(b) and 2(c), the displacement amplitudes at the two positions on the ground surface, i.e., (x_1/a, y_1/a) = (±1, 0), approach the value of 2 quickly as the source moves away. For another position under the ground surface in Fig. 2(d), the asymptotic values are 2 for horizontally and vertically incident cylindrical waves and around 1.211 for obliquely incident cylindrical waves, respectively. All of these asymptotic values are exactly

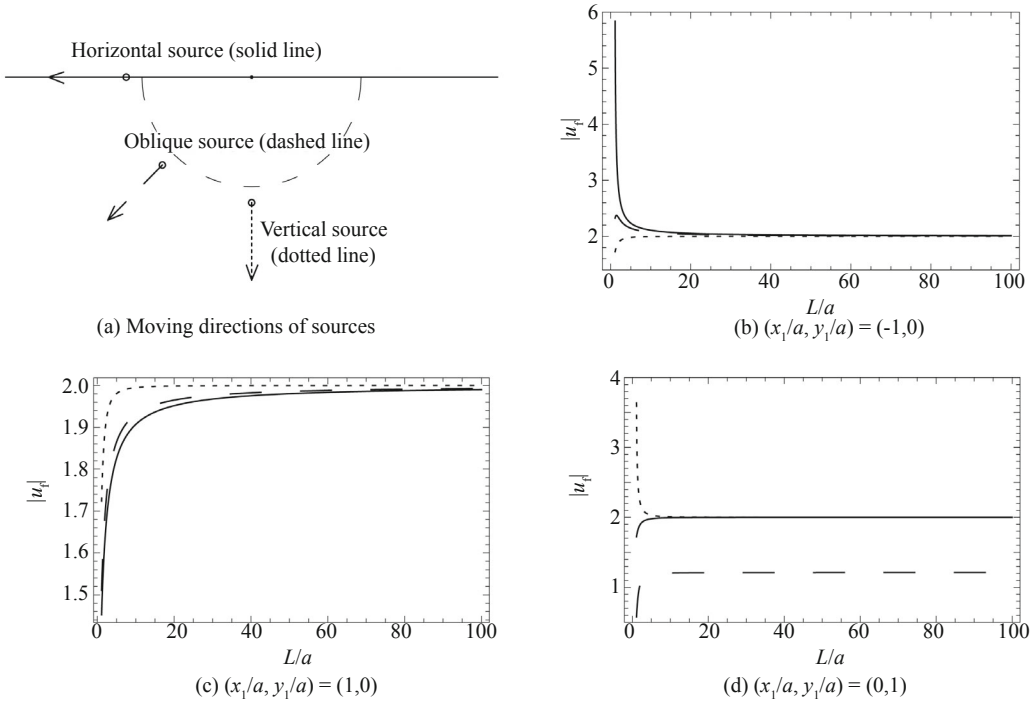

Fig. 2 Effects of dimensionless source distance L/a on the cylindrical-wave free-field displacement amplitudes $|u_t|$ at three positions $(x_1/a, y_1/a)$ for three moving directions of sources at $\eta = 1$

the plane-wave free-field displacement amplitudes (it can be obtained directly by the sum of Eqs. (8) and (9) in Tsaur and Chang (2008)). It can be concluded that the cylindrical-wave free-field approaches the plane-wave free-field very quickly at the three positions near the irregular site as the source moves away.

The second part of the wave field in Sub-region 1 is the scattered field generated by the alluvial valley as

$$u^s(r_1,\theta_1)=\sum_{n=0}^{\infty}A_n\mathrm{H}_{2n}^{(2)}(k_1r_1)\cos 2n\theta_1+\sum_{n=0}^{\infty}B_n\mathrm{H}_{2n+1}^{(2)}(k_1r_1)\sin(2n+1)\theta_1 \tag{12}$$

in which A_n and B_n are unknown complex coefficients.

According to Tsaur and Chang (2008), the transmitting wave in Sub-region 2 can be written in two different coordinate systems as:

$$u_2(r_2,\theta_2)=\sum_{n=0}^{\infty}C_n\mathrm{J}_{2n}(k_2r_2)\cos 2n\theta_2+\sum_{n=0}^{\infty}D_n\mathrm{J}_{2n+1}(k_2r_2)\sin(2n+1)\theta_2 \tag{13}$$

and

$$u_2(r_1,\theta_1)=\sum_{n=0}^{\infty}C_n\sum_{m=0}^{\infty}\mathrm{J}_m(k_2r_1)\mathrm{J}_{m,2n}^{+}(k_2d)\cos m\theta_1-\sum_{n=0}^{\infty}D_n\sum_{m=1}^{\infty}\mathrm{J}_m(k_2r_1)\mathrm{J}_{m,2n+1}^{-}(k_2d)\sin m\theta_1 \tag{14}$$

where C_n and D_n are the unknown complex coefficients, and the other symbols are identical to Tsaur and Chang (2008) as well.

Note that the difference between this study and Tsaur and Chang (2008) is the excitation of the model. Therefore, we can take advantage of the formulations proposed by Tsaur and Chang (2008) to solve the unknown constants, A_n, B_n, C_n and D_n herein. To avoid repetition, only the infinite systems of equations for C_n and D_n and the expressions of A_n and B_n in terms of C_n and D_n are listed here.

$$\sum_{n=0}^{\infty}C_n\sum_{m=0}^{\infty}\mathrm{J}_{m,2n}^{+}(k_2d)\left[\sum_{p=0}^{\infty}\mathrm{J}_m'(k_2a)I_{m,2p}^{C}(\beta)I_{2p,2q}^{C}(\beta)\frac{\varepsilon_p\mu_2\mathrm{H}_{2p}^{(2)}(k_1a)}{\pi\mu_1\mathrm{H}_{2p}^{(2)\prime}(k_1a)}-\mathrm{J}_m(k_2a)I_{m,2q}^{C}(\beta)\right]=\frac{2\mathrm{i}}{\pi a}\sum_{n=0}^{\infty}\frac{P_nI_{2n,2q}^{C}(\beta)}{\mathrm{H}_{2n}^{(2)\prime}(k_1a)}\qquad q=0,1,2\ldots \tag{15}$$

$$\sum_{n=0}^{\infty}D_n\sum_{m=1}^{\infty}\mathrm{J}_{m,2n+1}^{-}(k_2d)\left[\sum_{p=0}^{\infty}\mathrm{J}_m'(k_2a)I_{m,2p+1}^{S}(\beta)I_{2p+1,2q+1}^{S}(\beta)\frac{2\mu_2\mathrm{H}_{2p+1}^{(2)}(k_1a)}{\pi\mu_1\mathrm{H}_{2p+1}^{(2)\prime}(k_1a)}-\mathrm{J}_m(k_2a)I_{m,2q+1}^{S}(\beta)\right]=-\frac{2\mathrm{i}}{\pi a}\sum_{n=0}^{\infty}\frac{Q_nI_{2n+1,2q+1}^{S}(\beta)}{\mathrm{H}_{2n+1}^{(2)\prime}(k_1a)}\qquad q=0,1,2\ldots \tag{16}$$

$$A_n=\frac{\varepsilon_n\mu_2}{\pi\mu_1\mathrm{H}_{2n}^{(2)\prime}(k_1a)}\sum_{p=0}^{\infty}C_p\sum_{m=0}^{\infty}\mathrm{J}_m'(k_2a)\mathrm{J}_{m,2p}^{+}(k_2d)I_{m,2n}^{C}(\beta)-P_n\frac{\mathrm{J}_{2n}'(k_1a)}{\mathrm{H}_{2n}^{(2)\prime}(k_1a)}\qquad n=0,1,2\ldots \tag{17}$$

$$B_n = -\frac{2\mu_2}{\pi\mu_1 \mathrm{H}_{2n+1}^{(2)\prime}(k_1 a)} \sum_{p=0}^{\infty} D_p \sum_{m=1}^{\infty} \mathrm{J}'_m(k_2 a) \mathrm{J}^{-}_{m,2p+1}(k_2 d) I^{S}_{m,2n+1}(\beta) - Q_n \frac{\mathrm{J}'_{2n+1}(k_1 a)}{\mathrm{H}_{2n+1}^{(2)\prime}(k_1 a)} \qquad n = 0, 1, 2\ldots \tag{18}$$

At last, the numerical computation can be conducted after the truncation of the infinite series in Eqs. (15) through (18). The summation indexes n and p are truncated to N terms (i.e., $n = 0 - N\text{-}1$, $p = 0 - N\text{-}1$), and m is truncated to M terms (i.e., $m = 0 - M\text{-}1$ or $1 - M$). The unknown complex coefficients C_n and D_n can be obtained by solving the system of equations consisting of Eqs. (15) and (16) with standard matrix techniques. Afterwards, the coefficients A_n and B_n can be evaluated by means of the truncated Eqs. (17) and (18) in a straightforward way. Thus, the wave fields of a series form in each sub-region have been obtained.

Note that the values of N should be found by converging tests, and the M value should match the Eq. (15) in Tsaur and Chang (2008) accordingly. Figure 3 shows four examples of convergence tests for five representative points at $x_1 = -2a$, $-b$, 0, b, $2a$ on the ground surface. The chosen configuration is a partially filled alluvial valley with $h/a = 0.75$ subject to horizontal incidence. It can be seen that the convergence is strongly affected by the dimensionless frequency and slightly affected by the source position. Higher frequency cases require larger values of N. In general, for $N \leq 25$ and $M \leq 85$, it is enough to obtain the convergence of the results in this paper.

3 Numerical results and discussions

3.1 Normalized displacement amplitude

The displacement u of any particular location in the half-plane can now be obtained by using the theoretical formulations in Section 2. The amplitude of the complex-valued displacement u defined by Trifunac (1971) is adopted here:

$$|u| = \sqrt{\mathrm{Re}^2(u) + \mathrm{Im}^2(u)} \tag{19}$$

in which $\mathrm{Re}(\cdot)$ and $\mathrm{Im}(\cdot)$ denote the real part and imaginary part of a complex-valued function, respectively.

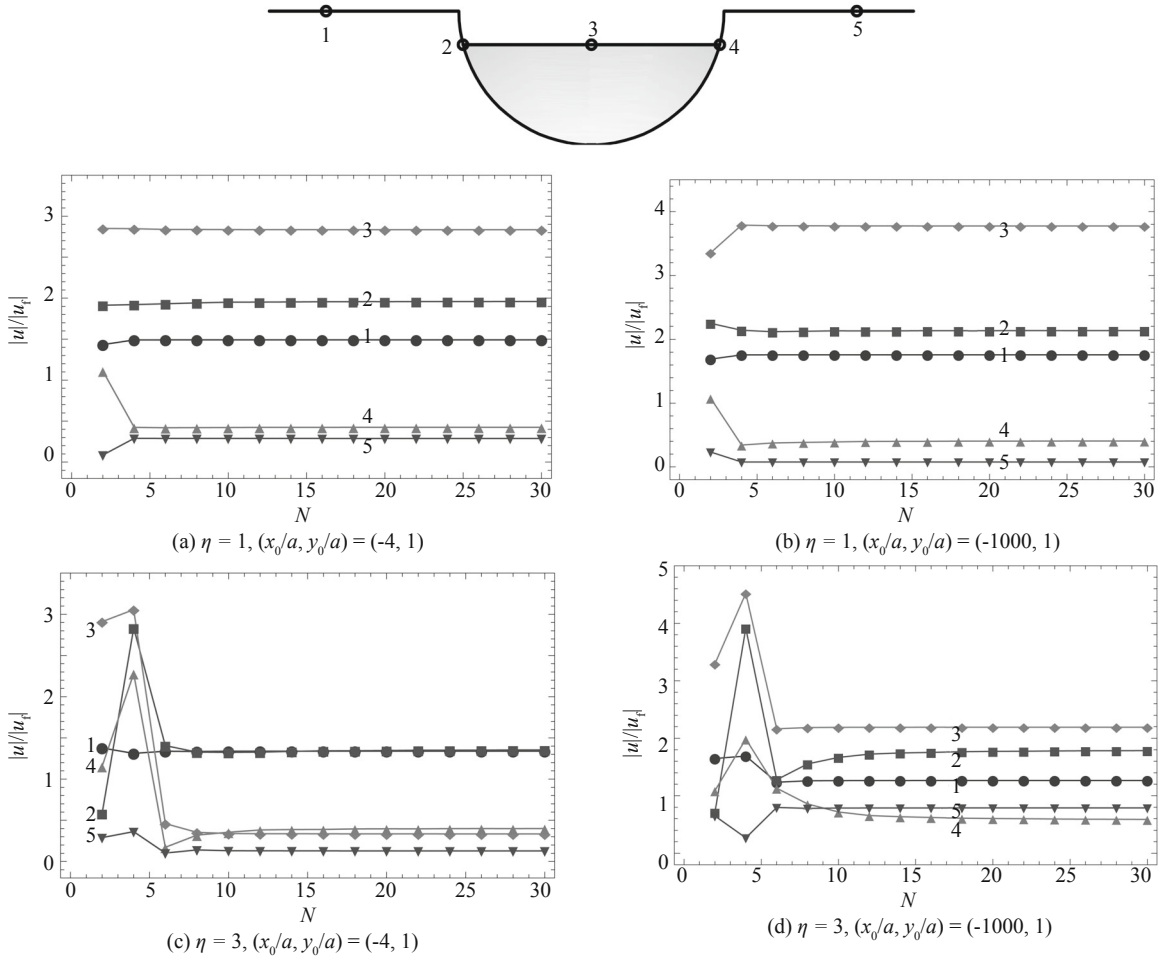

Fig. 3 Convergence test examples at five positions on the ground surface for a partially filled alluvial valley with $h/a = 0.75$

Generally, the site effect can be observed if one compares the displacement amplitude of a half-plane with irregularities to the displacement amplitude of the free field. The free-field displacement amplitude $|u^f|$ for different observation points on the ground surface is a constant number (twice the incident motion) for the case of plane-wave incidence, while it is not a constant number for the cylindrical-wave case (Eq. (3)). It is difficult to find the amplification pattern directly through the displacement amplitude under cylindrical-wave incidence. Thus, following Gao and Zhang (2013), the amplification factor is obtained by normalizing the displacement amplitude to the free-field amplitude, i.e., $|u_j|/|u^f|$. When the normalized displacement amplitude or amplification factor $|u_j|/|u^f|$ at a particular position is greater than 1, the ground motion at the position is amplified; on the contrary when it is smaller than 1, the ground motion is reduced.

For convenience, a dimensionless frequency is defined (see also, e.g., Trifunac (1971))

$$\eta = \frac{2a}{\lambda} = \frac{k_1 a}{\pi} \tag{20}$$

in which λ denotes the wavelength of the incoming wave.

3.2 Near-source versus far-field site effects

To validate the method proposed herein and reveal the relationship between the near-source and far-field site amplification effects, the cylindrical-wave results yielded by the theory presented herein needs to be compared with the plane-wave results in previous works. Following Trifunac (1971) and Tsaur and Chang (2008), the main parameters ρ_1/ρ_2, c_1/c_2, and μ_1/μ_2 of the model are set to be 1.5, 2.0 and 6.0, respectively. Note that the near-source site effect refers to the cylindrical wave results for a finite source-to-site distance in comparison to the plane wave results for an infinite distance.

Figure 4 demonstrates both the near-source amplification factors by our method (dotted and dashed lines) and the far-field results based on the methods in Tsaur and Chang (2008) (solid lines) for a partially filled alluvial valley with h/a = 0.5. Note that the alluvial valley ranges from x_1/a = -1 to x_1/a = 1. The amplification factors for nearby sources of cylindrical waves with $(x_0/a, y_0/a)$ = (0, 5), (-5, 5) and (-5, 1) differ from those for plane-wave cases. For example, the ground motions at x_1/a = ±3.5 in Fig. 4(a) and x_1/a = 0 in Fig. 4(f) are amplified for the plane-wave case but reduced for the cylindrical-wave case. Furthermore, the extent of the amplification or reduction may be modified with the change of wave types. A case in point is the horizontal incidence case at x_1/a = 0.5 in Fig. 4(c), where the amplification factor reaches around 6.1 under the excitation of plane waves, while it only reaches around 5.0 under the excitation of cylindrical waves. These results demonstrate the necessity of reconsidering the plane-wave assumption and taking the nearby sources into account in site effects.

It also can be seen from Fig. 4 that the amplification patterns for the cylindrical-wave sources $(x_0/a, y_0/a)$ = (0, 100), (-50, 50), and (-20, 1) (dashed lines) are in good agreement with those corresponding to plane waves (solid lines). That is to say, the near-source amplification factors for the vertical, oblique and horizontal incident cases agree well with the corresponding far-field ones if the source-to-site distance surpasses some value. These agreements indicate that, as expected, the far-field result is acceptable if the source locates very far away from the irregular sites. In addition, these kinds of agreements also indicate that there is no error in the theoretical formulations herein.

3.3 Near-source site effects

Actually, the source location is a key factor in the amplification patterns of the alluvial valley. Figures 5 and 6 demonstrate the influence of the dimensionless location $(x_0/a, y_0/a)$ of a single source on the site amplification factors. The only difference between the two figures is the different dimensionless frequencies η. The amplification factors keep changing along the ground surface, i.e., apparent oscillations along the curves of amplification factors can be easily observed in Figs. 5 and 6. The curves of amplification factors oscillate more frequently when the source distance increases. That means more amplifications and deamplifications will occur within the same range of ground surface if the source moves further from the alluvial valley. It also can be seen that the curve of amplification factors oscillates more frequently as the frequency increases from η = 1 in Fig. 5 to η = 3 in Fig. 6. Moreover, the frequency η plays a role in modifying the oscillatory amplitudes of the curves.

Particularly, for the cases of horizontal incidence in Figs. 5(c), 5(f), 5(i), 5(l), 6(c), 6(f), 6(i) and 6(l), the maximum of the amplification (at x_1/a = 0 to 1) increases with the source-to-valley distance. Considering that the plane wave is thought to be the limiting case of a cylindrical wave, this result can help understand the phenomenon in Figs. 4(c) and 4(f) that a plane wave generates larger maximum motions than a cylindrical wave does. In fact, the exact asymptotic equivalence between wave fields on the ground surface induced by plane and cylindrical waves has been derived in Section 2 when the source-receiver distances are large enough. Thus, the normalized response for a plane wave almost equals that for a cylindrical wave radiated by a source located at a very large distance away from the valley.

Figure 7 demonstrates that the site amplification effect of an alluvial valley can be influenced by the dimensionless distance x_1/a from the observation position to the center of the valley, the dimensionless source location $(x_0/a, y_0/a)$ and the dimensionless

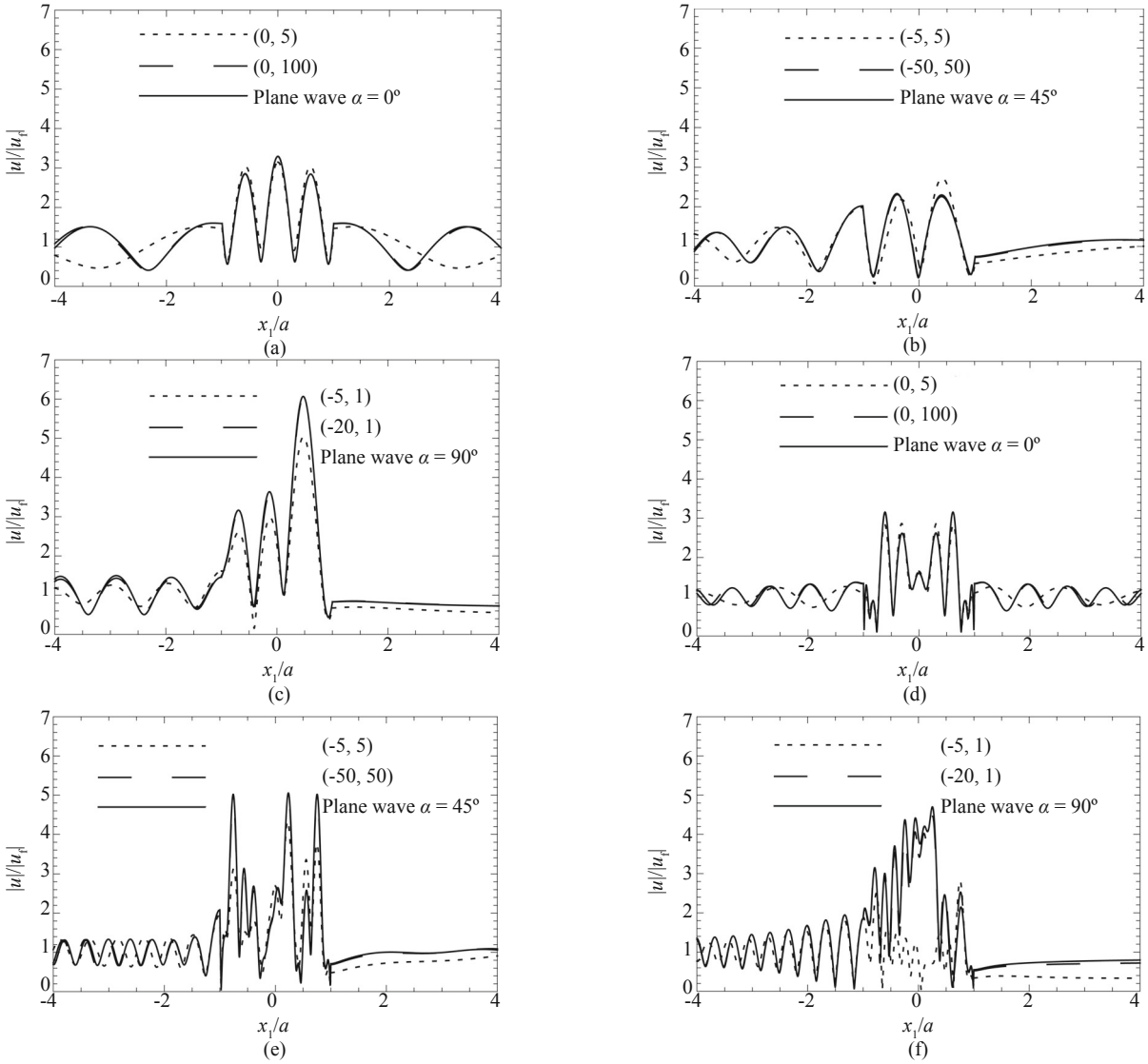

Fig. 4 Comparison of amplification factors for the cylindrical-wave incidence (near source) with those for the plane-wave incidence (far field) at h/a = 0.5. Dotted and dashed lines represent near-source results corresponding to different source locations (x_0/a, y_0/a) calculated by our method. Solid lines are far-field results corresponding to different incident angles α calculated by the method in Tsaur and Chang (2008). (a)-(c) η = 1, (d)-(f) η = 3

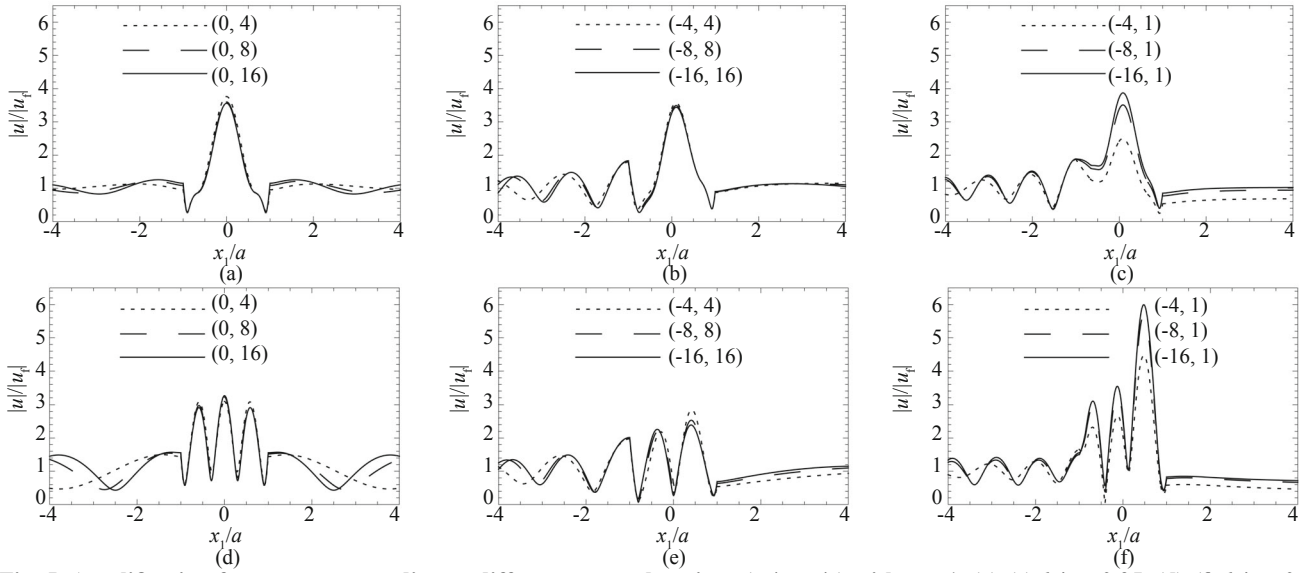

Fig. 5 Amplification factors corresponding to different source locations (x_0/a, y_0/a) with η = 1. (a)-(c) h/a = 0.25, (d)-(f) h/a = 0.5, (g)-(i) h/a = 0.75, (j)-(l) h/a = 1

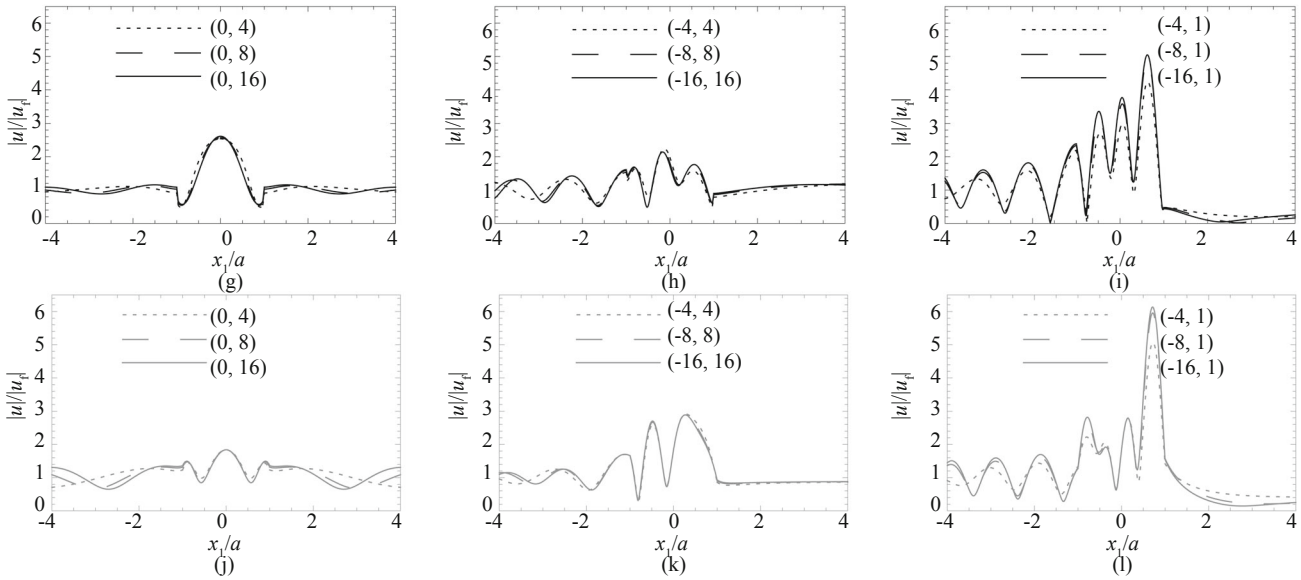

Fig. 5 Continued

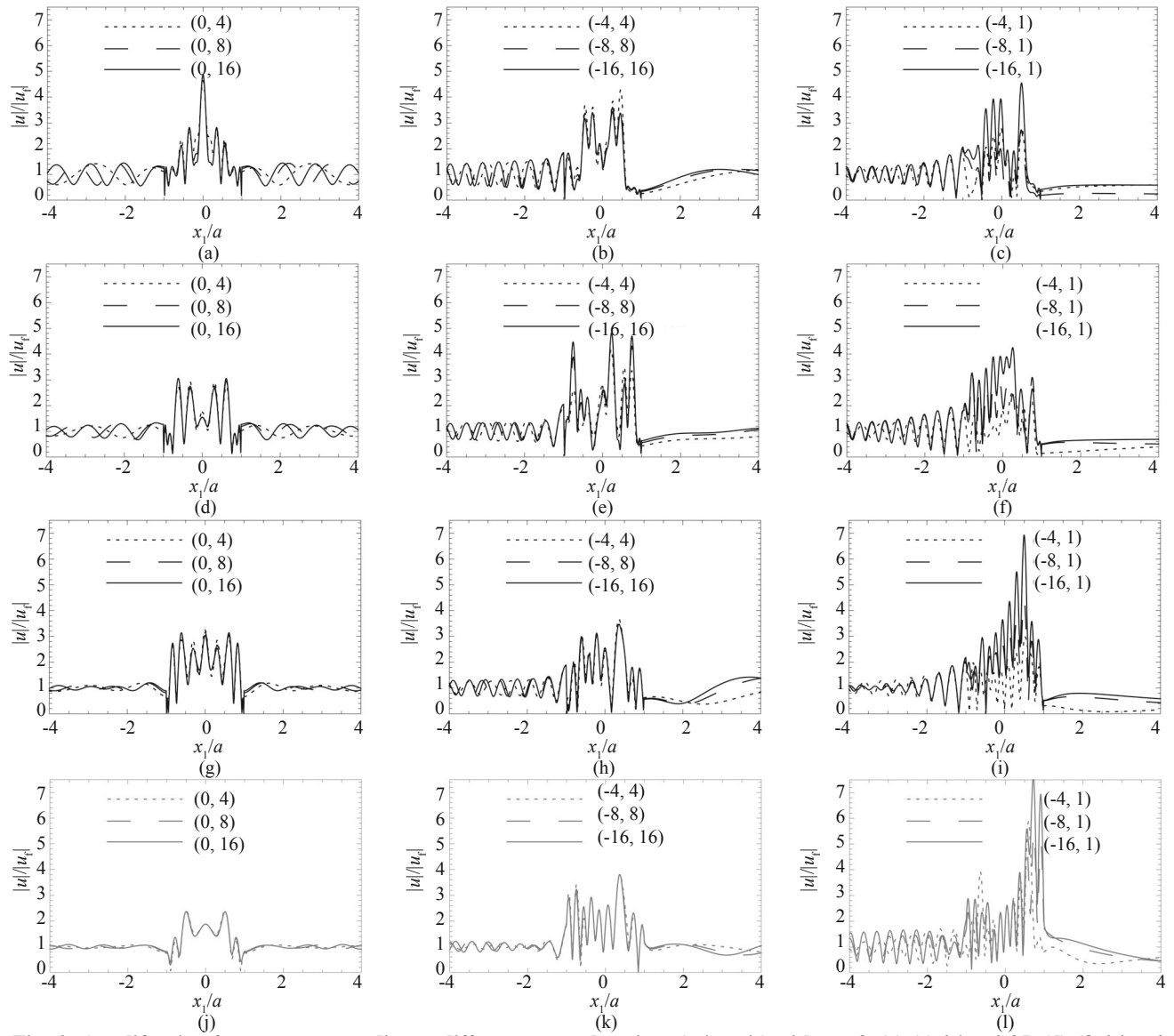

Fig. 6 Amplification factors corresponding to different source locations (x_0/a, y_0/a) with η = 3. (a)-(c) h/a = 0.25, (d)-(f) h/a = 0.5, (g)-(i) h/a = 0.75, (j)-(l) h/a = 1

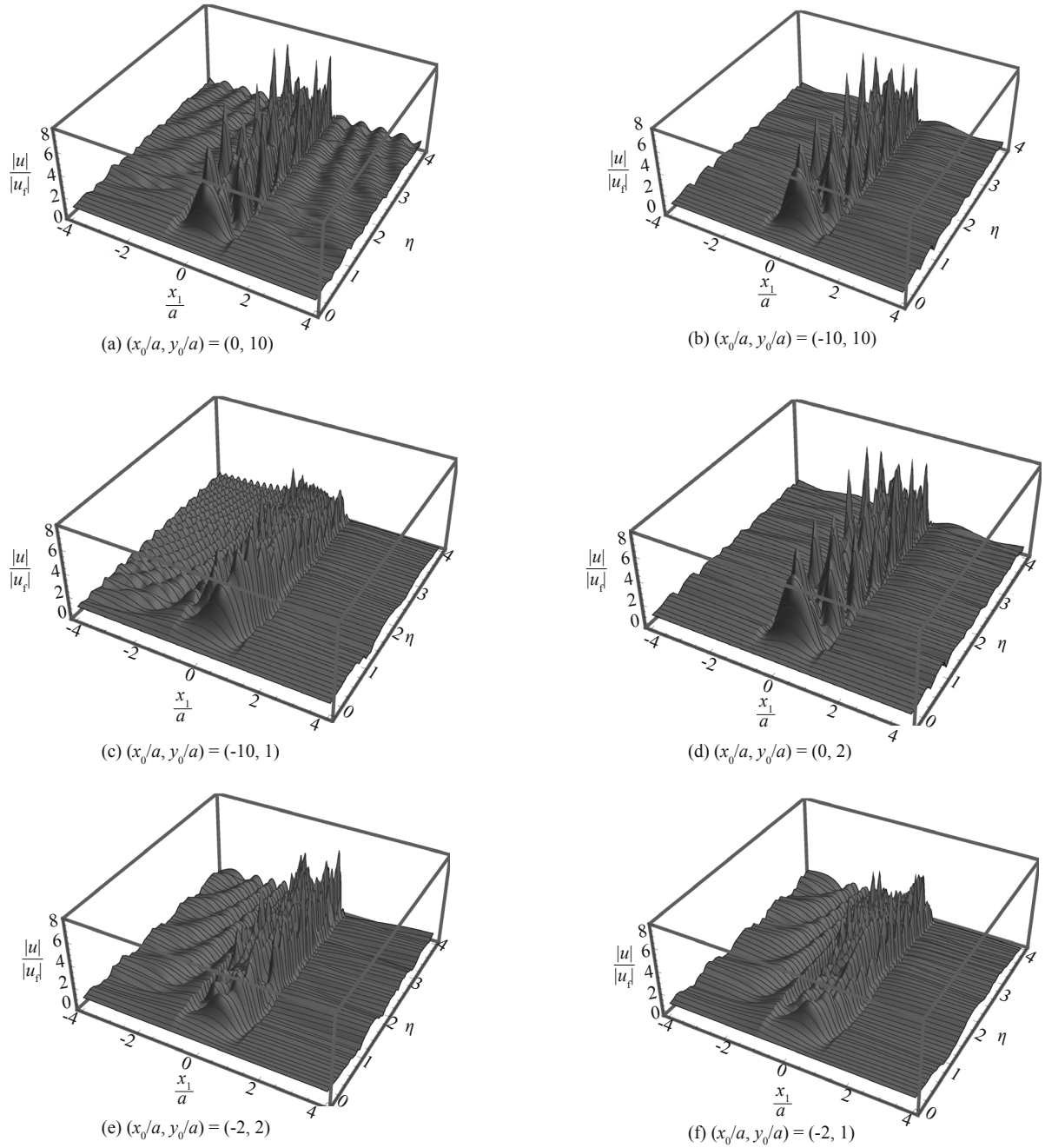

Fig. 7 3D plots of amplification factors as a function of x_1/a and η for a partially filled alluvial valley with h/a = 0.5 subjected to different sources

frequency η of the incident wave. In contrast to the near-source geometric amplification (Gao and Zhang, 2013), the maximum of the near-source site amplification is much larger and generally occurs within the range of the alluvial valley. Comparing Figs. 7(d), (e) and (f) to Figs 7(a), (b) and (c) respectively, it is found that the amplification patterns within the alluvial valley are only slightly different or even similar for different source distances, while the patterns outside the valley change significantly with source distances. The similarity within the valley may be due to the resonance nature of the dynamic response of the soil, which is less sensitive to the excitation. At the same time, the near-source effect dominates the ground motions outside the valley. That is to say, there will be less amplifications and deamplifications as the source moves closer to the irregular site (see also Figs 5 and 6).

Figures 8-10 show the time-domain results for h/a = 0.5. All parameters except source locations are kept identical to Figures 9(b) and 11(b) in Tsaur and Chang (2008). One can see the apparent curvature of the direct wave at about t = 5 s from Figs. 8(a) and 8(b) due to near-source effects. In contrast, Figs. 8(c) and 8(d) approach the case of plane wave in Figs. 9(b) and 11(b)

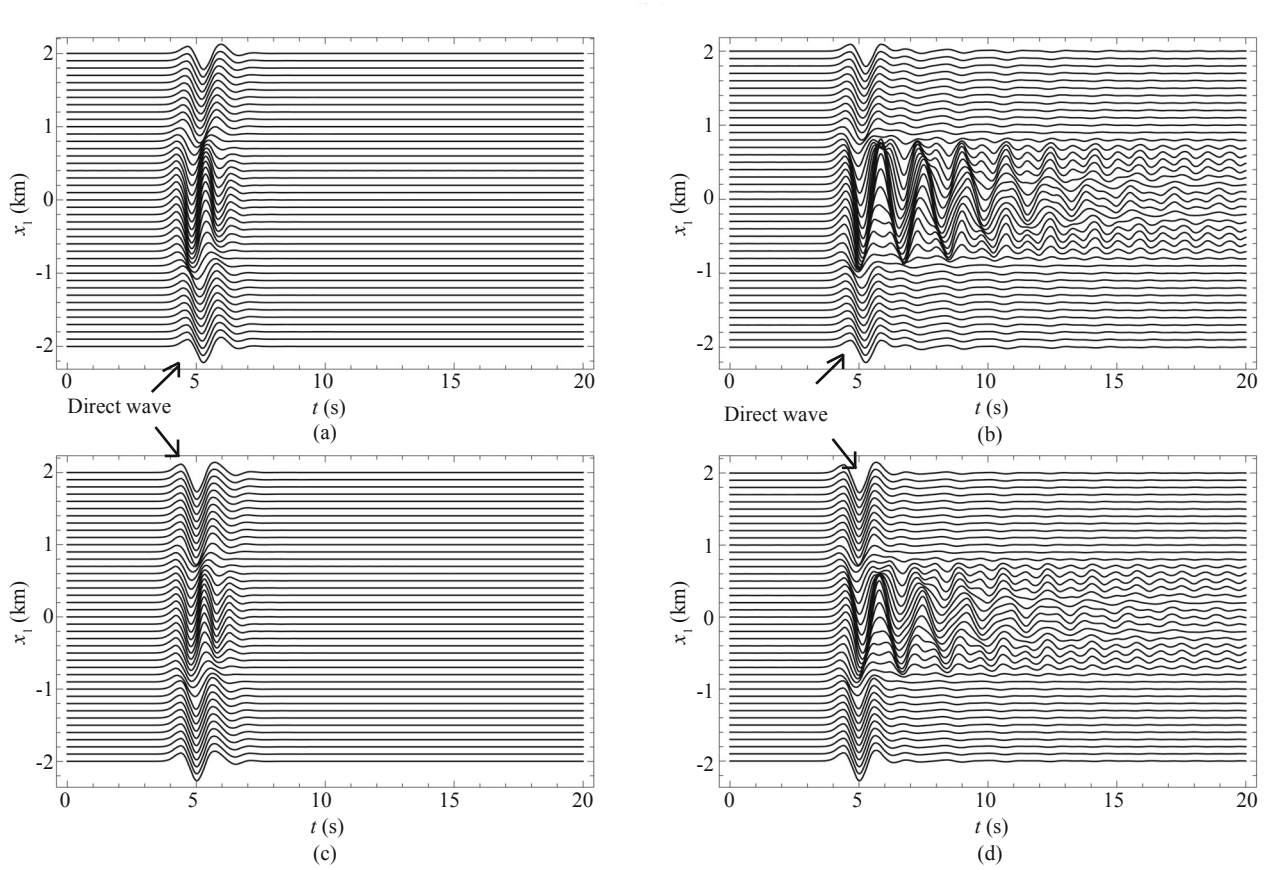

Fig. 8 Synthetic seismograms $u(x_1, t)$ for a partially filled alluvial valley with h/a = 0.5. (a) $(x_0/a, y_0/a)$ = (0, 2), c_1/c_2 = 1.5; (b) $(x_0/a, y_0/a)$) = (0, 2), c_1/c_2 = 3; (c) $(x_0/a, y_0/a)$ = (0, 100), c_1/c_2 = 1.5; (d) $(x_0/a, y_0/a)$ = (0, 100), c_1/c_2 = 3

in Tsaur and Chang (2008) because of a larger source-to-site distance. Taking a closer look, one can identify that the displacement amplitudes within the alluvial valley in Fig. 8(b) are larger than those in Fig. 8(d) due to stronger near-source effects (i.e., larger wave front curvature).

Figures 9 and 10 present the time-domain results for $(x_0/a, y_0/a)$ = (0, 5) and c_1/c_2 = 3, which shed some light on the physical process and mechanism of cylindrical SH wave scattering. In Fig. 9, the direct wave D1 can be identified clearly, which is the first wave received on the ground surface. One can see the obvious wave front curvature of the direct wave. Note that the direct wave reaches the position at about $x_1/a = \pm 0.87$ and y_1/a = 0.5 rather than the point at x_1/a = 0 and y_1/a = 0.5 at the earliest time because of the wave speed difference between the alluvial soil and its bedrock. The scattering waves within the alluvial valley are much bigger in amplitude and longer in duration time than those outside the valley due to the impedance ratio. In Fig. 10, the time-domain underground motions are in accordance with the ground motions in Fig. 9. The maximum motions at different times always take place within the alluvial valley after the direct wave passes away (Figs. 10(f)-(l); the brightest or darkest points).

One can see the main process of wave scattering by the irregular site in Fig. 10. At around t = 4.0 s, the direct wave D1 first arrives at the lower left and lower right corners of the valley (Fig. 10(a)). Then at t = 4.5 s and 5.0 s, the ground near the valley experiences motions induced by the direct wave. The reflection wave R1 appears afterwards as shown in Figs. 10(d) and (e). The first scattering wave S1 can be identified around the shoulders of the valley as the reflection wave R1 moves downwards (Fig. 10(e)). At t = 7.0 s and 7.5 s, the second

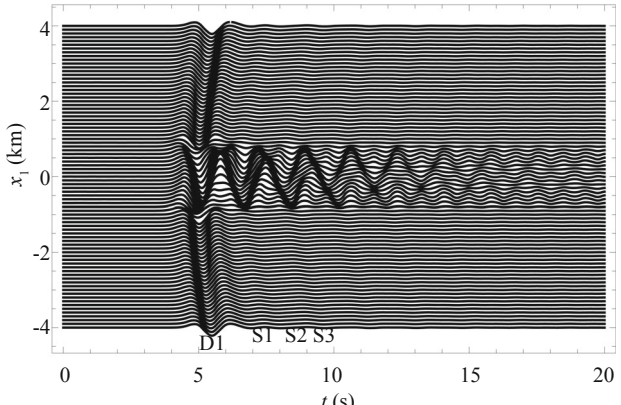

Fig. 9 Synthetic seismograms $u(x_1, t)$ for a partially filled alluvial valley with h/a = 0.5 for $(x_0/a, y_0/a)$ = (0, 5) and c_1/c_2 = 3

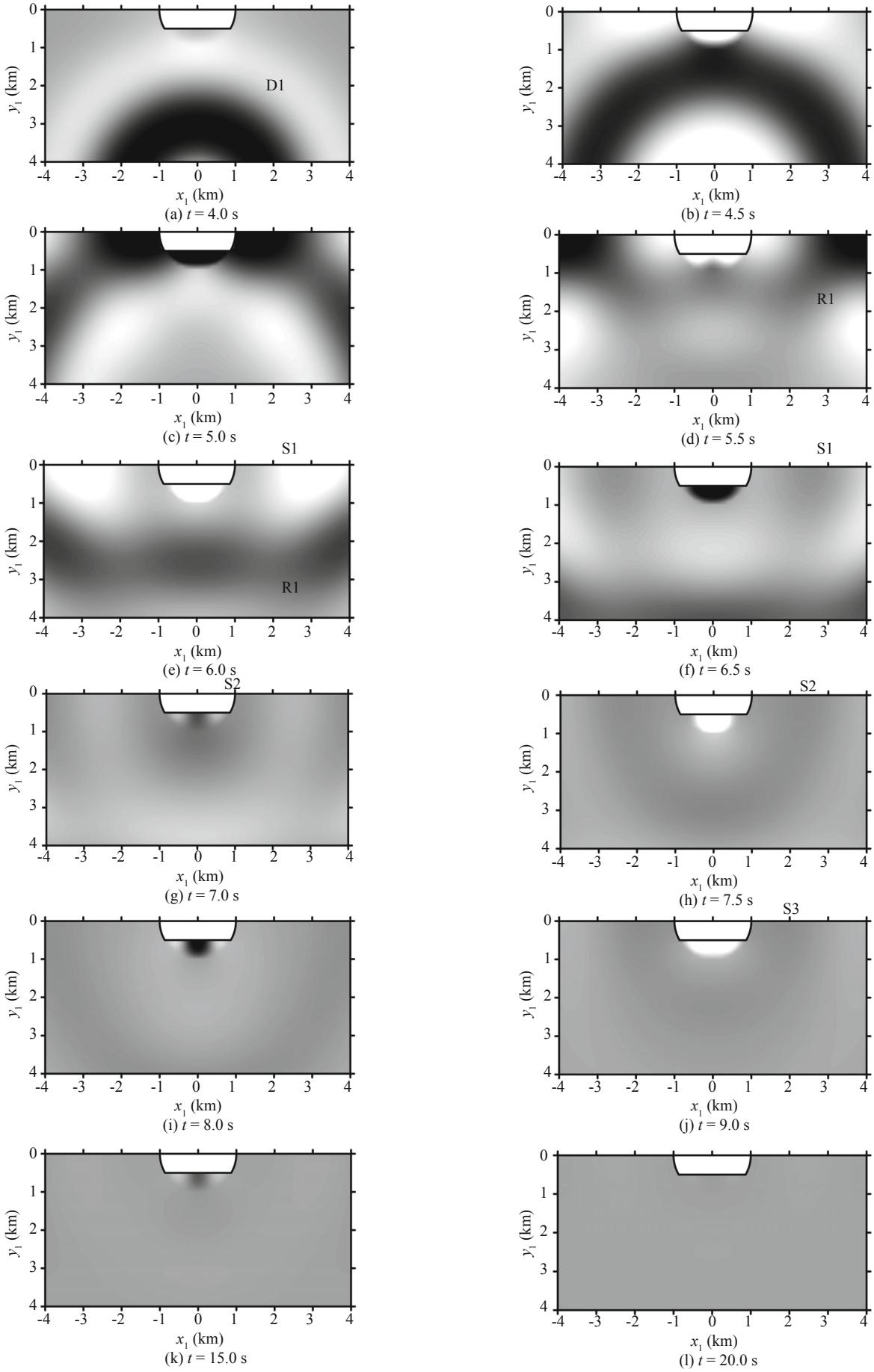

Fig. 10 Snapshots $u(x_1, y_1, t)$ at 12 specified times for a partially filled alluvial valley with $h/a = 0.5$ for $(x_0/a, y_0/a) = (0, 5)$ and $c_1/c_2 = 3$

scattering wave S2 occurs and propagates outwards (Figs. 10(g) and (h)). At t = 9.0 s, the third scattering wave S3 can be seen in Fig. 10(j). Note that there are more than three scattering waves. According to all the results in Fig. 10, the waves within the soft alluvial soil propagate back and forth and part of the energy stored in the soil will be released, inducing many scattering waves. It is hard to differentiate all of the scattering waves because of the decrease of their amplitudes. In Fig. 10(k), there are still wave motions in the valley but no obvious motion out of the valley. In Fig. 10(l), the energy stored in the valley finally dissipates through the bedrock.

4 Conclusions

An analytical series solution to the scattering of cylindrical SH waves induced by a partially filled semi-circular alluvial valley has been derived by using the wave function expansion technique. The results show that the source has a critical role in site effects. The responses at some positions may be amplified for plane-wave incidence but deamplified for the excitation of a nearby source of cylindrical waves. Furthermore, the source location plays a role in affecting the extent of the amplification or deamplification. Generally, there would be more amplifications and deamplifications of motions within a specified range of ground surface if the source moves further from the irregular site.

It is suggested that the traditional studies of site effects using the assumption of a plane wave incidence should be improved by including the influence of source characteristics. The theory proposed here may be applied to some engineering problems, for example, soil-structure interaction problems.

Acknowledgement

This research was supported by grants from National Natural Science Foundation of China (Grant Nos. 51479050 and 51338009), National Key Basic Research Program of China (Grant No. 2015CB057901), the Public Service Sector R&D Project of Ministry of Water Resource of China (Grant No. 201501035-03), the Fundamental Research Funds for the Central Universities (Grant Nos. 2013B05814, 2014B06814 and 2015B01214), and the 111 Project (Grant No. B13024).

References

Abramowitz M and Stegun IA (1972), *Handbook of Mathematical Functions, with Formulas, Graphs, and Mathematical Tables,* Dover, New York.

Boore DM (2004), "Can Site Response be Predicted?" *Journal of Earthquake Engineering*, **8**: 1–41.

Campillo M, Gariel JC, Aki K and Sanchez-Sesma FJ (1989), "Destructive Strong Ground Motion in Mexico City: Source, Path, and Site Effects during Great 1985 Michoacán Earthquake," *Bulletin of the Seismological Society of America*, **79**: 1718–1735.

Chaljub E, Moczo P, Tsuno S, Bard PY, Kristek J, Kaser M, Stupazzini M and Kristekova M (2010), "Quantitative Comparison of Four Numerical Predictions of 3D Ground Motion in the Grenoble Valley, France," *Bulletin of the Seismological Society of America*, **100**: 1427–1455.

Gao Y and Zhang N (2013), "Scattering of Cylindrical SH Waves Induced by a Symmetrical V-shaped Canyon: Near-source Topographic Effects," *Geophysical Journal International*, **193**: 874–885.

Gao Y, Zhang N, Li D, Liu H, Cai Y and Wu Y (2012), "Effects of Topographic Amplification Induced by a U-shaped Canyon on Seismic Waves," *Bulletin of the Seismological Society of America*, **102**: 1748–1763.

Groby JP and Wirgin A (2005), "Two Dimensional Ground Motion at a Soft Viscoelastic Layer/Hard Substratum Site in Response to SH Cylindrical Seismic Waves Radiated by Deep and Shallow Line Sources-I. Theory," *Geophysical Journal International*, **163**: 165–191.

Hough SE, Altidor JR, Anglade D, Given D, Janvier MG, Maharrey JZ, Meremonte M, Mildor BS, Prepetit C and Yong A (2010), "Localized Damage Caused by Topographic Amplification during the 2010 M 7.0 Haiti Earthquake," *Nature Geoscience*, **3**: 778–782.

Iturraran-Viveros U, Vai R and Sanchez-Sesma FJ (2010), "Diffraction of SH Cylindrical Waves by a Finite Crack: An Analytical Solution," *Geophysical Journal International*, **181**: 1634–1642.

Liang JW, Ba Z and Lee VW (2006), "Diffraction of Plane SV Waves by a Shallow Circular-arc Canyon in a Saturated Poroelastic Half-space," *Soil Dynamics and Earthquake Engineering*, **26**: 582–610.

Liang JW, Luo H and Lee VW (2004), "Scattering of Plane SH Waves by a Circular-arc Hill with a Circular Tunnel," *Acta Seismologica Sinica*, **17**: 549–563.

Liu DK and Han F (1991), "Scattering of Plane SH-wave by Cylindrical Canyon of Arbitrary Shape," *Soil Dynamics and Earthquake Engineering*, **10**: 249–255.

Lozano L, Herraiz M and Singh SK (2009), "Site Effect Study in Central Mexico Using H/V and SSR Techniques: Independence of Seismic Site Effects on Source Characteristics," *Soil Dynamics and Earthquake Engineering*, **29**: 504–516.

Luo H (2008), "Diffraction of SH-waves by Surface or Sub-surface Topographies with Application to Soil-structure Interaction on Shallow Foundations," *Report 248*, University of Southern California.

Luo H and Lee VW (2014), "Soil-structure Interaction on a Shallow Rigid Circular Foundation: SH Wave Source from Near-field Excitations," *Journal of Earthquake Engineering*, **18**: 67–89.

Mow and Pao (1971), "The Diffraction of Elastic Waves and Dynamic Stress Concentrations," *Report R-482-PR,* The Rand Corporation, Santa Monica, California.

Olsen KB (2000), "Site Amplification in the Los Angeles Basin from Three-dimensional Modeling of Ground Motion," *Bulletin of the Seismological Society of America*, **90**: S77–S94.

Olsen KB, Archuleta RJ and Matarese JR (1995), "Three-dimensional Simulation of a Magnitude 7.75 Earthquake on the San Andreas fault," *Science*, **270**: 1628–1632.

Parvez IA, Vaccari F and Panza GF (2006), "Influence of Source Distance on Site-effects in Delhi City," *Current Science*, **91**: 827–835.

Sanchez-Sesma FJ (1987), "Site Effects on Strong Ground Motion," *Soil Dynamics and Earthquake Engineering*, **6**: 124–132.

Sanchez-Sesma FJ, Palencia VJ and Luzon F (2002), "Estimation of Local Site Effects during Earthquakes: an Overview," *ISET Journal of Earthquake Technology*, **39**: 167–193.

Smerzini C, Aviles J, Paolucci R and Sanchez-Sesma FJ (2009), "Effect of Underground Cavities on Surface Earthquake Ground Motion under SH Wave Propagation," *Earthquake Engineering and Structural Dynamics*, **38**: 1441–1460.

Todorovska MI and Lee VW (1991), "Surface Motion of Shallow Circular Alluvial Valleys for Incident Plane SH Waves-analytical Solution," *Soil Dynamics and Earthquake Engineering*, **10**: 192–200.

Triantafyllidis P, Hatzidimitriou PM and Suhadolc P (2002), "Influence of Source on 2-D Site Effects," *Geophysical Research Letters*, **29**: 131–134.

Trifunac MD (1971), "Surface Motion of a Semi-cylindrical Alluvial Valley for Incident Plane SH Waves," *Bulletin of the Seismological Society of America*, **61**: 1755–1770.

Tsaur DH and Chang KH (2008), "SH-waves Scattering from a Partially Filled Semi-circular Alluvial Valley," *Geophysical Journal International*, **173**: 157–167.

Wang HY, Xie LL, Wang SY and Ye P (2013), "Site Response in the Qionghai Basin in the Wenchuan Earthquake," *Earthquake Engineering and Engineering Vibration*, **12**: 195–199.

Wong HL and Trifunac MD (1974), "Surface Motion of a Semi-elliptical Alluvial Valley for Incident Plane SH Waves," *Bulletin of the Seismological Society of America*, **64**: 1389–1408.

Yang ZL, Xu HN, Hei BP and Zhang JW (2014), "Antiplane Response of Two Scalene Triangular Hills and a Semi-cylindrical Canyon by Incident SH-waves," *Earthquake Engineering and Engineering Vibration*, **13**: 569–581.

Yuan XM (2014), "A Whole-space Transform Formula of Cylindrical Wave Functions for Scattering Problems," *Earthquake Engineering and Engineering Vibration*, **13**: 23–28.

Yuan XM and Liao ZP (1995), "Scattering of Plane SH Waves by a Cylindrical Alluvial Valley of Circular-arc cross-section," *Earthquake Engineering and Structural Dynamics*, **24**: 1303–1313.

Zhang N, Gao Y, Cai Y, Li D and Wu Y (2012a), "Scattering of SH Waves Induced by a Non-symmetrical V-shaped Canyon," *Geophysical Journal International*, **191**: 243–256.

Zhang N, Gao Y, Li D, Wu Y and Zhang F (2012b), "Scattering of SH Waves Induced by a Symmetrical V-shaped Canyon: A Unified Analytical Solution," *Earthquake Engineering and Engineering Vibration*, **11**: 445–460.